Production Engineering (2021) 15:457–466
https://doi.org/10.1007/s11740-021-01018-6

PRODUCTION PROCESS

# Decision basis for multi-directional path planning for post-processing reduction in material extrusion

**Steffen Hohenstein[1] · Georg Bergweiler[1] · Gerret Lukas[1] · Viktoria Krömer[1] · Tobias Otten[1]**

Received: 9 September 2020 / Accepted: 6 January 2021 / Published online: 19 March 2021


**Abstract**
Reducing support structures in Material Extrusion (ME) of Additive Manufacturing enables lowered post-processing efforts and enhanced use in industrial applications. This study provides a decision basis for multi-directional path planning strategy to print parts on multi-axis printers without the use of support structures. Research solutions for different limitations of ME systems are examined. The combination of Flat and Curved Layer Slicing, Adaptive Slicing, Load-Capable Path Planning and Multi-Axis Slicing enables printing a multi-directional demonstrator part. The part's build structure consists of form elements (features) with varying build directions depending on the transition areas between them. A proof-of-concept on a three-axis printer shows the ability of a multi-directional printing method for multi-axis printer systems. Interfaces between features require print parameter adjustment to obtain the desired mechanical properties. Tensile tests are performed to evaluate the mechanical load capacity at connecting areas between features of standard specimens. Geometrically complex parts (3D) are printed in conventional ME systems without support and improved characteristics through the multi-feature path planning strategy. Each feature is printed according to geometrically determined requirements representing a successful proof-of-concept. Results show that further testing is required for the effects of mechanical resistance at connection areas. Adaption of the path planning strategy is needed to reduce occurring defects.

**Keywords** Material extrusion · Pellets · 3 + 2 axis printing · Multi-directional path planning · Multi-axial printing · Post-processing

## 1 Introduction

The demand for shorter product development cycles poses challenges to today's production technologies. Modern production technologies must be flexible, economically efficient and enable reduced production times. Additive Manufacturing (AM) as an evolving production technology helps to overcome these challenges. AM facilitates the layer-wise generation of parts [1]. Its benefits for industrial use are the reduction of product development time, increased customization possibilities and freedom of design with almost no extra cost [2, 3].

Material Extrusion (ME), usually a filament-based AM technology for thermoplastics, has been established due to simple mechanisms, low asset costs and continuous material supply. It enables producing parts quickly and cost-efficiently [4]. However, three-axis ME printers commonly face multiple challenges. First, the isotropic tensile strength of parts demands a varying build direction [5]. Depending on the build orientation, geometric features such as overhangs necessitate support structures [6]. Around 26% of part costs in AM are generated in post-processing which represents an essential economic incentive. Zhao et al. [7] have a shown that the elimination of support structure and reduced stair-step effects result in less post-processing efforts regardless of the post-processing strategies applied [8, 9]. Most of the efforts in post-processing occur in removal of support material, such as breakaway in case of a dual extruder using PLA as a main material. Currently, AM for end-use applications is not utilized to its full potential, which could be changed through a feature-based printing approach.

In this study, a path planning strategy for multi-directional printing is developed and applied. The methodology developed in research and development (R&D) aims at reducing additional efforts in post-processing of printed

✉ Steffen Hohenstein
s.hohenstein@wzl.rwth-aachen.de

[1] Werkzeugmaschinenlabor der RWTH Aachen, Aachen, Germany

parts. The scientific benefit of the paper consists of analysis and utilization of significant slicing methods and optimized path planning strategies for multi-directional printing. In the first step of the multi-directional path planning strategy, the part's partial volumes are analyzed according to geometric characteristics. A systematic approach classifies the part according to its complexity, expressions, position and orientation. Each partial volume results in a feature with an assigned build direction. Building on the part's morphology, solutions for slicing and printing of each feature can be found. Previous research examines solution approaches to encounter specific limitations of three-axis printers such as reducing stair-step effects, eliminating support structures and enhancing a part's strength. However, it does not take the interdependencies between restrictions into consideration. Therefore, this study proposes a holistic approach that sets out to integrate selected existing approaches such as s Flat and Curved Layer Slicing (FCLS), Adaptive Slicing (AS), Multi-Axial Slicing (MAS) and Load Capable Path Planning (LCPP). These strategies only focus on single and isolated improvements, such as stair-case effects, mechanical characteristics and support-structures. In this context, feature printing makes use of one or a combination of multiple approaches. Extrusion path, build-up direction and reference levels are set for each feature individually. This study represents a decision aid for automated path planning in multi-feature printing based on expert knowledge.

The remaining part of the paper is structured as follows. The state of the art is presented in the following chapter and characterizes the material extrusion in additive manufacturing with layer modeling. Based on the characterization, restrictions of ME three-axis-printers show the demand for solutions approaches for product-orientated slicing in AM, which are described in Sect. 2.2.

The methodology in Sect. 3 enables suitable solution identification based on feature characteristics for printing. A fictional assembly tool functions as a demonstrator part for manual-based multi-feature path planning strategy in Sect. 4 and makes use of the developed methodology. The investigation of feature printing highlights the critical transition areas between features. Therefore, printing tensile specimens with various orientations of features facilitates the analysis of tensile strengths. Finally, the results of multi-feature printing and required next steps are discussed in Sect. 5.

## 2 State of the art

### 2.1 Material extrusion in additive manufacturing with layer modeling

Currently, ME is the main AM technology in industry use due to low investment costs for material and machines [1]. In the context of polymer AM, ME comprises plasticizing, extrusion and deposition of molten thermoplastics [10].

The principle underlying a filament-based ME process (ME-F), is shown in Fig. 1. Coiled filament is used as feed material. It is conveyed into the print head through feed rolls. The electrically heated nozzle transfers the filament into a viscous state by heating it close to its melting temperature [8, 9]. The filament is extruded through the nozzle and deposited on the build platform in strands where it solidifies. After the completion of a layer, the print head or substrate table move in z-direction by one layer height. [11]. The process is repeated until the part is completed. Overhangs require support structures. Usually, less than 45° means the application of support structure which is independent of materials. If multiple nozzles are available, different feed materials can be used for the part and support structures [8, 12].

Low extrusion rates and restricted material range for ME-F lead to the use of pellet-based extrusion principles [13, 14]. Current R&D machines underline the necessity of a product-orientated multi-feature printing method to reduce manual post-processes and reach required part properties, such as anisotropic properties and reduced surface roughness compared to conventional production technologies.

### 2.2 Restrictions of ME three-axis printers and solution approaches

Despite many benefits, the necessity of support structures, occurring stair-step effects and anisotropy limit three-axis ME printers to an isolated solution in production environment [15]. There are various approaches to eliminating these limitations while keeping the part's geometry unaltered. Instead of pursuing efforts in redesign of existing parts for AM, slicing methods should enable product-orientated printing. Flat and Curved Layer Slicing (FCLS) and Adaptive Slicing (AS) intend to reduce stair-step effects while Load-Capable Path Planning (LCPP) focuses on the part's anisotropy for better characteristics. Multi-Axial Slicing (MAS)

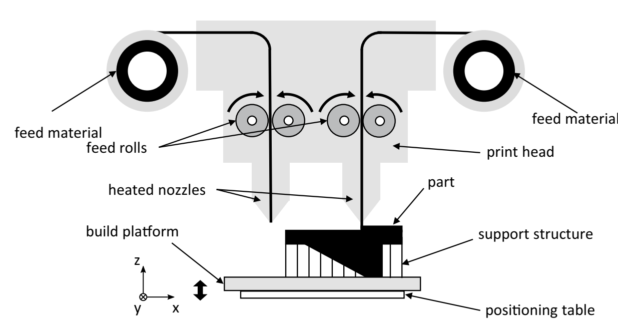


**Fig. 1** Principle of Fused Layer Modeling

was developed to reduce the number of support structures needed.

The FCLS algorithm by Huang and Singamneni divides parts into curved and flat layers preventing stair-step effects on curved surfaces. The algorithm slices external areas of the part into curved layers while internal areas are sliced in flat layers. To avoid sagging in strands along a curved path above a flat layer, the algorithm determines the number of curved layers necessary to avoid sagging of the top layer. A part that has been sliced into curved and flat layers can be seen in Fig. 2a [16] . FCLS eliminates any stair-step effects occurring on the outer surface. However, inner stair-step effects emerge, reducing the strength between flat and curved layers [16].

Through AS, areas vulnerable for stair-step effects are identified and sliced into layers with decreased layer thickness to minimize stair-step effects (see Fig. 2b). Stair-step effects can be reduced, but not eliminated by AS. Sikder et al. reduce the print time while improving the part's surface quality through decreasing the layer thickness by 20–40% with their algorithm [17].

LCPP utilizes anisotropy to improve strength properties. wulle et al. optimize mechanical properties of parts in an approach through utilizing the scaffolds in inner cavities of dense volumes. Their algorithm for multi-axial printing determines a tool path for internal structures of parts based on stress curves. The tool path is planned according to build directions of subdivided volumes and a part-specific stress curve. Application of the algorithm leads to improved mechanical resistance by factor 1.4 [18].

Parts can be built in multiple directions through MAS by dividing parts into areas with varying build orientations. A MAS algorithm by Ding et al. allows printing overhangs without support structures. The algorithm defines the print order of subdivided partial volumes and assigns a build direction to each. The ideal build direction is orthogonal to the area stretched by the normal vectors of the surfaces (see Fig. 2c). For gravitational reasons, the extrusion unit is orthogonal to the printing platform. This ensures a continuous material output to form an even layer, where print parameters can be adjusted in the same way as in the conventional process. While support structures can be minimized, the algorithm cannot be used for parts without defined concave edges. [19].

Zhao et al. present a comprehensive review of common slicing strategies. These strategies only focus on single and isolated improvements, such as stair-case effects, mechanical characteristics and support-structures [8].

The presented solution approaches represent the short-term goal for a product-orientated print method. In the long term, these principles should be referenced to decision conditions based on expert knowledge for an automated path planning combined with adjusted print parameters. The multifarious solutions enable a competitive production of polymer parts with AM.

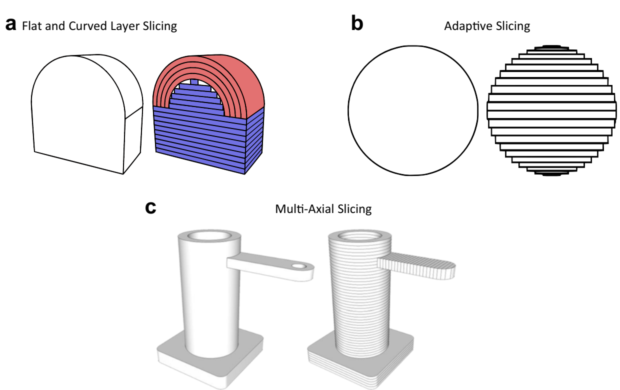


**Fig. 2** FCLS (**a**), AS (**b**) and MAS (**c**) with original part (left) and sliced part (right)

## 3 Methodology

The multi-directional path planning starts with the analysis of the part's partial volumes. Geometric characteristics provide information on the complexity degree of each partial volume and represent the requirements for the feature's print method. A systematic approach as shown in Table 1 is introduced to deduce print methods for features according to their morphological categories.

Defined basic elements consisting of shape (2D) and extrusion line (3D), e.g. cylinder or cuboid should be identified in features of the part to establish singular print methods. Element transitions or aggregated structures in more complex features are composed of these basic elements. The

**Table 1** Schemes for feature morphology and print method

| Feature | Geometric Characteristics | | | Solutions | Activities |
|---|---|---|---|---|---|
| *n* | Level 1 | Level 2 | Level 3 | | |
| | Type of feature | Expressions | Position & orientation | MAS<br>AS<br>FCLS<br>LCPP | e.g. modification of the G-Code |

second level are expressions, such as curvatures, curves and subtractions. Furthermore, the third level represents the positioning and orientation of the expressions. Finally, the description of the feature's morphology enables the application of solutions for multi-directional printing (Table 2).

FCLS, AS, and MAS are considered most suitable to be used in a combined approach to solve the limitations of ME. FCLS eliminates outer stair-step effects and is compatible with other solutions. Despite the occurrence of inner stair-step effects, FCLS affects the part stability positively. AS reduces the stair-step effects but does not eliminate it. It is fully compatible with other solutions. Further, print time can be reduced. MAS facilitates support-free printing, additionally, it avoids stair-step effects. However, due to varying build directions it does not combine limitlessly with other approaches.

While these approaches pose solutions to eliminate or reduce support structures and stair-step effects, none of them aims at reducing or seizing a part's anisotropy for mechanical properties. For this reason, LCPP is also included in the combined solution approach.

Part of the multi-directional path planning strategy is the subdivision of a component into partial volumes, where each has an individual build direction. The investigation clarifies the difference between two slicing strategies, which are a 2.5D (uni-directional) and 3D print method (multi-directional). Information contained in the model history and software solutions are used to detect features. Build directions are allocated according to direction of leading line, extrusion path and reference level. Single use or a combination of the solutions introduced above are applied to each feature depending on the geometric requirements. The implemented strategy leads to the multi-directional, build-up structure. Tensile strength of the feature interfaces is evaluated on the Ultimaker Original +. The investigation on a three-axis printer represents a preliminary manual-based study for printing geometrically complex parts on multi-axis printers. Within feature printing slicing methods are used, however an automated print in one-step is not possible due to limited degree of freedom of the three-axis printer. By using the following slicing methods printing of an assembly tool is enabled for e.g. a five-axis printer moving the part in its horizontal orientation of the transition area for each feature.

## 4 Multi-directional printing—Implementation on an assembly tool and tensile testing

The focus of this study lays on the methodology approach of multi-directional printing. At first, the multi-directional printing of an assembly tool on a three-axis printer is deduced underlining the challenges of feature-orientated printing (cf. chapter 4.1). Subsequently, the mechanical strength of the interfaces between features represents the main focus of chapter 4.2 Tensile strength must be tested to detect mechanical vulnerability of multi-directional printed parts. While the path planning and printing process parameters are adapted, the parts' geometry is kept unaltered. Hereafter, multi-directional printing of an assembly tool on a three-axis printer is deduced and tensile strength between features examined on standard specimens according to DIN EN ISO 527-2.

### 4.1 Multi-directional assembly tool

The design of the fictional demonstrator tool requires the use of support structures and results in stair-step effects if printed layer-based on a regular three-axis ME printer. Multi-directional printing of the part prevents these effects. Based on expert knowledge, the part is manually subdivided into four features as described above. Current R&D efforts deal with automated detection of features within parts. The assembly tool, resulting features, belonging base areas and build directions are depicted in Fig. 3.

An overview of the geometric challenges occurring in each feature as well as chosen solutions and activities is given in Fig. 3 and further described in detail below. Collision avoidance in multi-directional printing plays a

**Table 2** Overview of features and solution approaches

| Feature | Geometric Characteristics | Solutions | Activities |
|---|---|---|---|
| 1 | None | None needed | Automatic G-code generation by conventional slicer |
| 2 | Extrusion path with different cross sections | MAS<br>AS<br>LCPP | G-Code modification<br>Adaption of extrusion factor<br>Recording of force progression<br>Reinforcement through part filling |
| 3 | Axis of the hole not parallel to build direction<br>Curved surface not in a plane perpendicular to the print head | AS<br>FCLS | Slicing in curved and flat layers and layers of varying height<br>Adaption of the extrusion factor |
| 4 | Different build direction than previous feature | MAS | Manual turning and fixture of feature 3 on build platform |

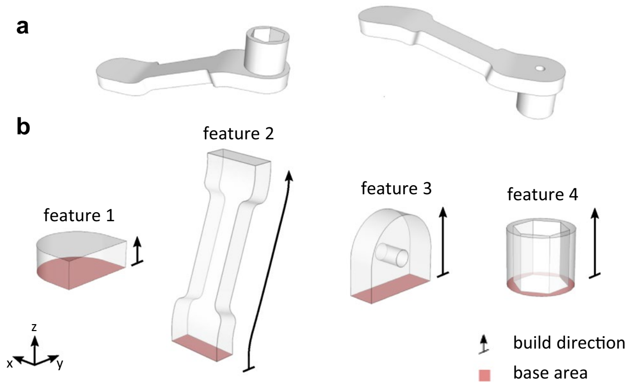


**Fig. 3** Assembly tool (**a**), features in build order from left to right (**b**)

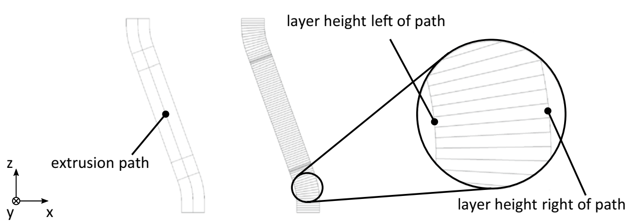


**Fig. 4** Slicing of feature 2 along the extrusion path

significant role determining base areas and printer head accessibility. This study focuses on the print sequence for entire parts. Feature 1, 2, and 3 are each printed separately. Feature 4 is printed on the final plane of feature 3.

Feature 1 is sliced conventionally, transferred into a G-code and printed without further actions due to a simple geometry (2.5D) free of overhangs and curved areas. Feature 1 is followed by feature 2 with a different build direction. If printed on top of each other on a multi-axis printer, the part must be turned until the new build direction is parallel to the print head. For this purpose, the G-code must contain information about build direction and address additional motion axes, e.g. rotational axes.

Feature 2 contains different cross sections along the extrusion path. The slicing software must slice the feature accordingly. The resulting layers with partially varying layer height within themselves are shown in Fig. 4.

To provide the necessary amount of material in every position of each layer and avoid material gaps and impoundment, the extrusion factor must be modified. It is defined by the ratio of material feed and length of the deposited strand. The cross section of a deposited plastic strand in this feature can be described by means of an isosceles trapezium as in Fig. 5. The following Eq. (1) is set up to determine the extrusion factor depending on the trapezoidal center.

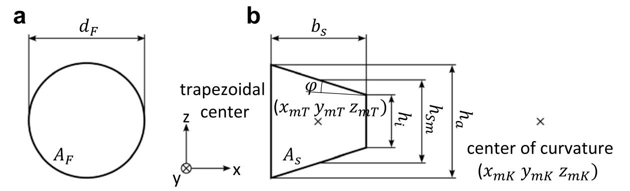


**Fig. 5** Cross sectional areas of filament (**a**) and deposited strand (**b**)

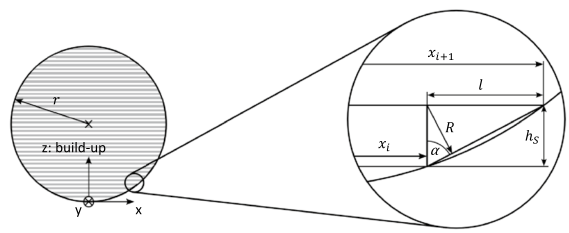


**Fig. 6** Determination of the roughness value

$$E = \frac{8\pi b_S \left(x_{mK} - x_{mT}\right)\tan(\varphi)}{d_F^2} \tag{1}$$

$b_S$ = width of deposited strand. $x_{mK}$ = x-coordinate of center of curvature. $x_{mT}$ = x-coordinate of trapezoidal center. $\varphi$ = angle between two adjacent layers. $d_F$ = filament diameter. $A_F$ and $A_S$ refer to the cross-sectional areas of the feed material and deposited strand. The outer, mean and inner height of the trapezoid base are termed $h_a$, $h_{Sm}$ and $h_i$. The y- and z-coordinates of the trapezoidal center and center of curvature are described as $y_{mT}$, $y_{mK}$, $z_{mT}$, $z_{mK}$.

Feature 2 is reinforced through internal part filling according to LCPP. Force progression is determined, and the highest force identified at the end of the lever. For ideal force absorption, the structure of the infill is orientated perpendicular to the force direction.

Feature 3 resembles feature 1 geometrically except for a cylindrical hole. However, feature 3 is built in a different direction as the final plane of feature 2 functions as the base area for feature 3. Due to the given orientation, the axis of the cylindrical hole is not parallel to the build direction. As a result, stair-step effects occur. In order to reduce these stair-step effects, AS is applied. Adherence to a given roughness value ensures the hole's functionality. In this feature, due to layers with uniform layer height within themselves, the cross section of a deposited plastic strand is described as a rectangle. Equation (2) is set up to determine the extrusion factor.

$$E = \frac{4b_S h_S}{\pi d_F^2} \tag{2}$$

$h_S$ = layer height of deposited strand. $b_S$ = width of deposited strand. $d_F$ = filament diameter.

The roughness value is established depending on the layer height according to Eq. (3) in compliance with Fig. 6.

$$R = \frac{\sqrt{r^2 - (y_{i+1} + h_s - r)^2} - \sqrt{r^2 - (y_i - r)^2}}{\sqrt{\left(\frac{\sqrt{r^2-(y_{i+1}+h_s-r)^2}-\sqrt{r^2-(y_i-r)^2}}{h_s}\right)^2 + 1}} \tag{3}$$

$h_S$ = layer height of deposited strand. r = circle radius. $y_i$ = height of layer i. $y_{i+1}$ = height of layer i + 1.

The distance between the circle center and -contour of layer i is termed $x_i$. Based on the circular equation, the x-distance between two adjacent layers $x_i$ and $x_{i+1}$, distance *l* is measured.

Due to the build orientation, the curved surface of feature 3 is not in a perpendicular plane to the print head. FCLS is applied to prevent stair-step effects that occur along the surface if printed layer-based. The curved surface is offset by ten layers and curved instead of flat layers are used (cf. Fig. 7). Due to the printing capabilities of the Ultimaker Original+, only around one third of the surface is offset and printed with curved layers in practice. Usual printer heads have limited ability to print curved layers because of embedded nozzles. Ultimaker Original+ has a non-embedded nozzle and enables collision-free printing of curved layers.

Feature 4 has a different built direction than feature 3. On a multi-axial printer, the part would be rotated to orientate the base area of feature 4 perpendicular to the nozzle. On the Ultimaker Original+, the part is manually removed from the build platform, turned by 90° and attached to the build platform again. Ensuing, feature 4 is printed on feature 3 resulting in bonding of the features.

The composed tool is displayed in Fig. 8. Feature 1 and 2 are separated, feature 3 and 4 are joined. Each feature is realized without support structures under consideration of its geometric characteristics. Air gaps occur on the outer side of the curvature of feature 2 under the usage of an angle of 0.5° between two adjacent layers. In feature 3, material deferall occurrs along the curved layers. Due to the kinematic capabilities of the used three-axis system, the features of the assembly tool are printed separately for verification of the multi-directional slicing strategy. The features are bonded subsequently to visualize the entire assembly tool. Tensile strength of features joined by direct printing is tested separately on standardized multi-directional specimens.

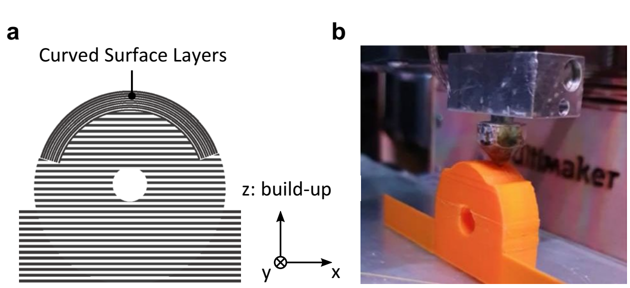


**Fig. 7** **a** Curved Layer Printing principle. **b** Practical printing test specimen

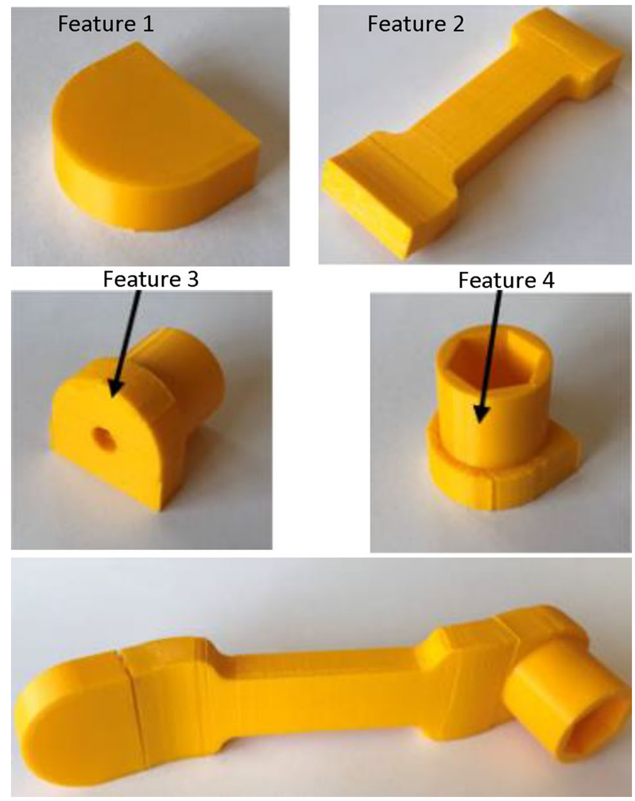


**Fig. 8** Multi-feature printed assembly tool

## 4.2 Tensile testing on multi-directional standard specimens

Tensile strength of multi-directional PLA specimens is tested to evaluate mechanical weakness between features. Specimens are printed according to DIN EN ISO 527–2 on the same printer as the assembly tool. Testing takes place on a Z250 SN AllroundLine by ZwickRoell. The specimens consist of two grip sections (feature 1 and 3) and the testing area (feature 2) in between. The build orientation of the layers in feature 2 differs from the grip sections. Inclination angles between 0° up to 90° in intervals of 15° between feature 1 and 2 are investigated. Five specimens of each of seven types (SM1–SM7) are printed, one of which (SM1)

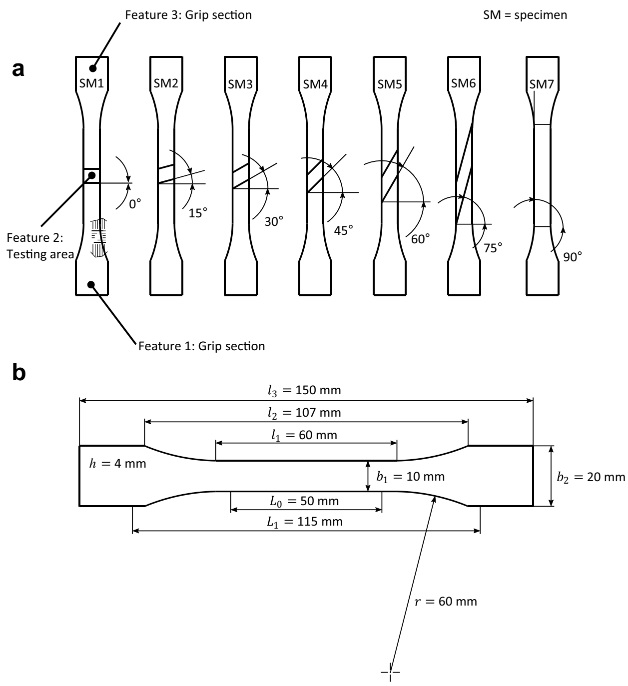


**Fig. 9** Specimens with differently angled testing areas (**a**) and dimensions according to DIN EN ISO 527–2 (**b**)

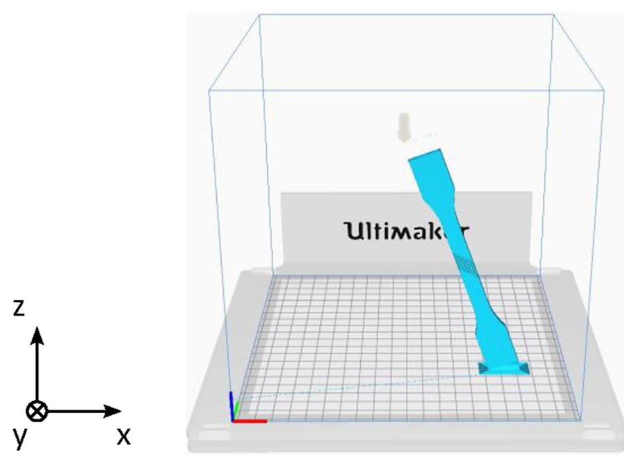


**Fig. 10** Orientation of samples on the build platform

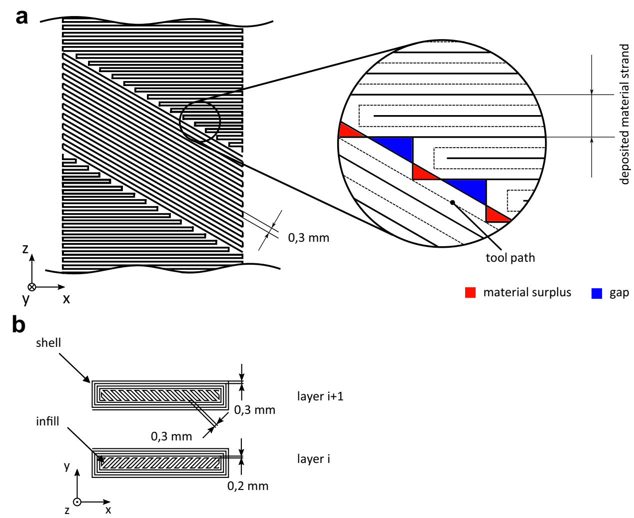


**Fig. 11** Path planning strategy (top) and layer design (bottom)

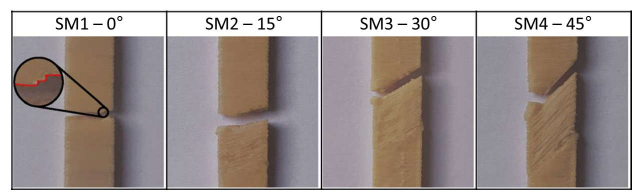


**Fig. 12** Breakage behavior of SM1–SM4

functions as a reference specimen due to the same build orientation in all areas (c.f. Fig. 9).

To simulate multi-directional printing on multi-axis printers best possibly on a three-axis printer, the specimens are printed standing upright to recreate geometrical restrictions such as overhangs. Safe standing is ensured through edging the outer filling of the layer twenty times (see Fig. 10).

The transition between grip sections and testing area is aimed to be filled volumetrically: The tool path of the testing area is set up so that the outer edge of the deposited material strand intersects the edges of the material strands in the grip sections. The extrusion factor is kept constant, leading to extruded material where strands have already been deposited in the previous layer. The arising material accumulation is supposed to move into the gaps caused by the tool path as displayed in Fig. 11. No material is extruded during movement of the print head between two parallel strands to avoid unnecessary material accumulation.

Following parameters are set to provide high strength of each layer: The shell consists of four lines, each offset by 0.3 mm. Infill consists of parallel paths, each also offset by 0.3 mm and rotated by 45° in relation to the shell. After each layer, infill orientation changes by 90°. Distance between shell and infill is set to 0.2 mm. The path planning strategy and layer design are shown in Fig. 11.

Layers in the testing area inclined by 30° or more suffer from insufficient quality due to collision with the print head and gravitation reasons. The entire specimens are rotated around the y-direction and reoriented on the build platform. The procedure enables multi-directional printing and almost a horizontal starting plane for the inclined feature in the middle of the tensile probe. After the final printing process, tensile strengths of the specimens with layers inclined by more than 45° (SM5—SM7) are too poor (below 2 MPa) to be considered in the tensile strength testing. Tensile strength of

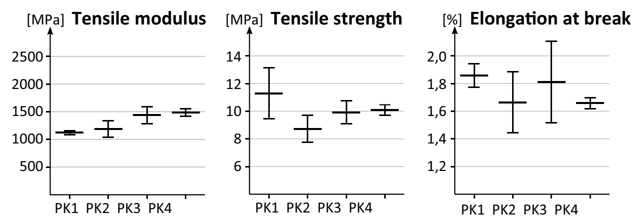


**Fig. 13** Statistical analysis of the breakage behavior

the specimens of SM1—SM4 is tested according to DIN EN ISO 527-2. Preload force is determined and set to 1.17 MPa. Results of the breakage behavior can be seen in Fig. 12.

Notches arise in all specimens. The higher the angle between the different structural alignments, the greater the notch. All samples of the reference specimen SM1 break inside the testing area through multiple layers. One of five samples of SM2 shows breakage along the separating layer except for a fringe that is not broken along the separating layer. The other four samples show breakage outside the testing area. Unlike SM2, all samples of SM3 are broken along the separating layer, each with a fringe that shows breakage on the x–y-plane. The breakage behavior of the samples of SM4 is analogue to that of the samples of SM3. The statistical assessment of the tensile modulus, tensile strength and elongation at break of the tensile specimens is shown in Fig. 13.

Samples of the reference specimen SM1 show highest average tensile strength. Change in structural alignment of the testing area results in lower tensile strength. The higher the inclination angle, the higher the resulting tensile modulus. The influence of the inclination angle on the elongation at break cannot be determined with the examined test results.

## 5 Discussion and outlook

In this study, multi-directional printing of parts printed on a ME printer is introduced. Based on other authors' research, a methodology is developed giving instructions on how to set up path planning for features that a part is subdivided into. The path planning is built on geometric characteristics of each feature. Application takes place on a fictional assembly tool divided into four features and printed feature-based. Mechanical weakness between features is expected due to anisotropy resulting in tensile strength testing of multi-feature standard specimens according to DIN EN ISO 527-2.

The path planning strategies of the four features of the tool are individually generated based on the solution approaches. It is printed on a three-axis kinematics system, the Ultimaker Original +, without the use of support structures. Features 1–3 are printed separately whilst feature 4 is printed on top of feature 3. Despite reduced stair-step effects and increased quality, challenges occur during the printing process: As MAS is used to realize different cross sections along the extrusion path in feature 2, air gaps on the outer side of the curvature emerge. It is derived that the angle between two adjacent layers must be sufficiently small when using MAS along an extrusion path. Otherwise, the distance becomes too large to ensure adherence between the layers. When applying FCLS along curved layers in feature 3, material deferall occurs due to the curved surface not in a perpendicular plane to the print head. Further, collision free printing is only possible on the Ultimaker Original + through offsetting one third of the planned surface. The use of a multi-axis printer would enable differing orientations of print head or build platform to ensure perpendicularity and collision free offsetting of the entire surface. Tensile strength is tested on multi-feature standard specimens according to DIN EN ISO 527–2 whose features are joined directly during the printing process. The extrusion factor is kept constant during the printing process of the specimens. A volumetric filling in the transition between grip sections and testing areas is strived through including intersections of deposited material strands in the tool path. Resulting gaps in the transition area are compensated with surplus material. It is unclear to what extent the surplus material does fill in the resulting gaps and if the approach affects the strength between features. New challenges exist in printing a new layer (feature n + 1) on the rough surface of feature n (cf. Fig. 14). Depending on the inclination angle of the testing area, the ratio between material surplus and gaps is unequal. Further research demands the realization of the transition between features with an adapted extrusion rate. The provision of the exact amount of needed material along the tool path gives further information about the mechanical strength between features.

As expected, tensile strength testing of the parts printed with a uniform extrusion rate reveals mechanical vulnerability between connected features. While breakage often occurs within the testing area along the separating layer, it passes from the separating layer to the x–y-plane in fringes. This is caused by the deposition of multiple small layers in the peripheral areas. Layers cool down only for a short time span before the following layer is deposited. Consequently, the temperature level is increased leading to strong merger

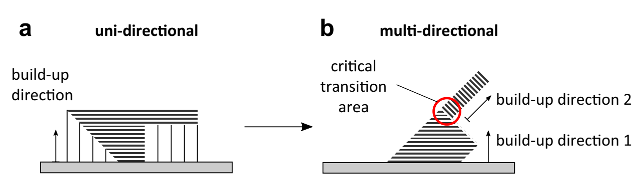


**Fig. 14** **a** Uni-directional slicing; (**b**) Multi-directional slicing with critical transition area between features

of the surrounding layers and high strength. Mechanical vulnerability between features can be counteracted through optimal merger of the deposited layers. There are several hypotheses, which represent further research steps. The first hypothesis is that at the connection areas the physical joining becomes weaker. The second hypothesis states that if the angle becomes more oblique, the weakened area is significantly larger and therefore a larger force can be transmitted. However, shear and tensile stresses occur in the layer resulting in a different stress condition. Merger can be reached through slow material deposition including long linger of the hot nozzle at connecting areas or through heating of the separating layer before depositing a new layer, causing a high temperature level.

The proof-of-concept on a three-axis ME printer shows the possibilities to apply multi-directional printing on multi-axis printer systems. In further research, the introduced path planning strategy must be applied to a part that is subsequently printed on a five-axis printer. Nevertheless, five-axis printers cannot be applied in arbitrary ways. This approach enables the validation of the path planning strategy and integrated tensile strength testing of joined features, possibly needing adaption. Detected challenges occurring during the printing process described above must be eliminated: The angle between two adjacent layers should be decreased when applying MAS to determine if air gaps reducing adherence still occur. The print head needs to be oriented perpendicular to curved surfaces when using FCLS to avoid material deferral. The extrusion factor for the path planning in transition areas in specimens must vary to ensure the right amount of material along the tool path. It should be tested if the modification affects the mechanical strength between features compared to a constant extrusion rate. Further adaption of the parameter set to reach higher merger as described above needs to take place and must be quantified with tensile tests.

The introduced concept shows how to enhance the use of ME in industrial applications. The developed methodology enables support-free printing whilst achieving better part quality and strength. The fulfilment of mechanical requirements and less post-processing efforts make ME economically more efficient for industrial use. The next research steps are the inductive establishment of print methods for features based on their morphological characteristics.

**Funding** Open Access funding enabled and organized by Projekt DEAL.



## References

1. VDI Verein Deutscher Ingenieure (2014) VDI-Richtlinie 3405. Additive Fertigungsverfahren—Grundlagen, Begriffe, Verfahrensbeschreibungen. Beuth, Berlin
2. Gebhardt A, Hötter J.-S (2016) Machines for rapid prototyping, direct tooling and direct manufacturing. In: Additive manufacturing. 3D printing for prototyping and manufacturing, 5.th ed. Carl Hanser, München, pp 232–235
3. Hopkinson N, Hague R.J.M, Dickens P.M (eds) (2005) Unlocking the design potential of rapid manufacturing. In: Rapid manufacturing. An industrial revolution for the digital age. John Wiley, Chichester, p 5
4. Kumar N, Jain PK, Tandon PM (2018) Extrusion-based additive manufacturing process for producing flexible parts. J. Braz. Soc. Mech. Sci. & Eng. 40(3):1–12. https://doi.org/10.1007/s40430-018-1068-x
5. Wohlers Associates I (ed) (2017) Wohlers report 2017. 3D printing and additive manufacturing state of the industry—annual worldwide progress report. Wohlers Associates, Fort Collins, p 191
6. Gibson I, Rosen DW, Stucker B (2010) Extrusion-Based Systems. Additive Manufacturing Technologies: Rapid Prototyping to Direct Digital Manufacturing. Springer, Boston, pp 144–152
7. Wohlers associates (2019) Wohlers report 2019: additive manufacturing and 3D printing state of the industry; annual worldwide progress report, p. 140
8. Zhao D, Guo W (2020) Mixed-layer adaptive slicing for robotic Additive Manufacturing (AM) based on decomposing and regrouping. In: J Intell Manuf (Journal of Intelligent Manufacturing) 4.th edn.
9. Deutsches Institut für Normung (2017) DIN EN ISO/ASTM 52900:2017-06. Additive Fertigung—Grundlagen—Terminologie. Beuth, Berlin, p 8
10. Gebhardt A, Hötter J. S (2016) Basics, Definitions and Application Levels. In: Additive Manufacturing. 3D printing for prototyping and manufacturing, 5.th edn. Carl Hanser, München, p 14
11. Gibson I, Rosen D, Stucker B (2015) Extrusion-Based Systems. In: Additive Manufacturing Technologies. 3D Printing, Rapid Prototyping, and Direct Digital Manufacturing, 2nd edn. Springer, New York, p 157
12. Volpato N, Kretschek D, Foggiatto JA (2015) Experimental analysis of an extrusion system for additive manufacturing based on polymer pellets. INT J ADV MANUF TECH 81(9–12):1519–1531. https://doi.org/10.1007/s00170-015-7300-2
13. Klapproth K (2017) Study Shows Tamping Better for BAAM. https://chemical-materials.elsevier.com/new-materials-applications/study-shows-tamping-baam/. Accessed 07 Oct 2018
14. Wulle F, Coupek D, Schäffner F, Verl A, Oberhofer F, Maier T (2017) Workpiece and machine design in additive manufacturing for multi-axis fused deposition modeling. Procedia CIRP 60:229–234. https://doi.org/10.1016/j.procir.2017.01.046
15. Huang B, Singamneni S (2015) A mixed-layer approach combining both flat and curved layer slicing for fused deposition modelling. Proc IMechE Part B 229(12): 2238–2249 doi: https://doi.org/10.1177/0954405414551076
16. Sikder S, Barari A, Kishawy H (2015) Global adaptive slicing of NURBS based sculptured surface for minimum texture error in rapid

prototyping. Rapid Prototyping J 21(6):649–661. https://doi.org/10.1108/RPJ-09-2013-0090
17. Wulle F, Wolf M, Riedel O, Verl A (2019) Method for load-capable path planning in multi-axis fused deposition modeling. Procedia CIRP 84: 335–340. Doi: https://doi.org/10.1016/j.procir.2019.04.188
18. Ding D, Pan Z, Cuiuri D, Li H, Larkin N, van Duin S (2016) Automatic multi-direction slicing algorithms for wire based additive manufacturing. Robot Cim-Int Manuf 37:139–150. https://doi.org/10.1016/j.rcim.2015.09.002
19. Grutle K (2015) 5-axis 3D Printer. Designing a 5-axis 3D printer. Master thesis, University of Oslo